IOPscience iopscience.iop.org

Home Search Collections Journals About Contact us My IOPscience

Evidence for a surface resonance feature in the very low-energy electron spectrum of ZrN

This article has been downloaded from IOPscience. Please scroll down to see the full text article.

1991 J. Phys.: Condens. Matter 3 S207

(http://iopscience.iop.org/0953-8984/3/S/033)

View the table of contents for this issue, or go to the journal homepage for more

Download details:
IP Address: 129.252.86.83
The article was downloaded on 27/05/2010 at 11:24

Please note that terms and conditions apply.

J. Phys.: Condens. Matter 3 (1991) S207–S216. Printed in the UK

Evidence for a surface resonance feature in the very low-energy electron spectrum of ZrN

P T Dawson, K K Tzatzov and Y Chen
Department of Chemistry and Institute for Materials Research, McMaster University, Hamilton, Ontario, L8S 4M1, Canada

Received 25 April 1991

Abstract. Previous investigations of the low-energy (0–40 eV) electron spectra of Ti and V nitrides have been extended to ZrN. The low-energy spectra of ZrN films prepared by nitrogen ion implantation contain the corresponding features to those previously observed for TiN and VN. However, the ZrN spectrum is dominated by an extremely large feature at about 3 eV, which has not been previously reported. The amplitude of this peak varies directly with the nitrogen concentration. The peak shape and intensity are sensitive to primary electron beam energy in the range 0.5 to 2.0 keV, but the peak position does not change. The strong dependence of the amplitude of this feature on physisorption of gases and crystallorgraphic orientation suggest that this peak arises from structure in the secondary electron spectrum induced by a surface resonance.

1. Introduction

The transition metal nitrides form a series of interesting materials with interesting physical and chemical properties, and also important technological applications [1]. Previous work has reported on the low energy electron spectra of titanium and vanadium nitrides in which the problem of the disappearance of the Auger transitions between 20 and 30 eV initiated by creation of a metal p vacancy [2,3] was explained by the identification of two new Auger transitions at even lower energy, about 5 and 15 eV, arising from N(2s) and M(3p) holes respectively [4].

The present work is our first report on the extension of these studies to the related zirconium nitride system. At first sight the results obtained bore striking similarities to those previously observed for Ti and V, particularly in the intensity pattern observed for the Zr(4p)Zr(4d)Zr(4d) and Zr(4p)N(2p)Zr(4d) transitions at 23 and 19 eV. However, when looking for the comparable transitions to those observed in TiN and VN at still lower energies, our attention was drawn to a remarkably strong feature, near 3 eV in the $dN(E)/dE$ spectrum. The peculiar behaviour of this feature, including its sensitivity to gas adsorption and crystallographic orientation, will be the subject of this paper.

2. Experimental methods

A zone-refined zirconium rod was sliced into a sample disk 12 mm in diameter and 1 mm thick, mechanically polished, finally with 1 μm diamond paste, solvent degreased

and transferred to ultra high vacuum. The sample was cleaned by alternate argon ion sputtering and annealing until no impurities could be detected by AES. Sputtering was performed using a rastered 2 kV argon ion beam directed at 80 degrees to the surface normal, and using a standard argon pressure of 5×10^{-5} torr, the ion beam current density, measured with a Faraday cup, was approximately 50 μA cm^{-2}.

Zirconium nitride films were prepared in situ by ion implantation of nitrogen ions with energies in the range of 3 to 5 kV. Previous experience with titanium and vanadium nitrides prepared in this manner showed that this procedure produced films with a composition close to stoichiometric.

Auger electron spectra were obtained in the derivative mode using a four-grid retarding potential electron energy analyser. The primary 2 kV, 25 μA electron beam of 0.1 mm diameter was directed normal to the sample surface. The spectra were acquired digitally and the spectrometer was controlled by a microcomputer. The low (0–50 eV) energy electron spectrum was measured with a modulation voltage of 1 V peak-to-peak and a sweep resolution of 0.1 eV, taking eight samples at each energy. The nitrogen KLL, zirconium MNN and potential impurity Auger peaks, C, O, S, P, etc, were measured with a sweep resolution of 0.5 eV and a modulation of 10 V p–p.

Gas pressures are reported as uncorrected nitrogen equivalent pressures measured using a standard ion gauge. The gas purity was monitored with a 1–200 amu quadrupole mass spectrometer.

3. Results

3.1. Low energy electron spectra of ZrN and Zr

The secondary electron spectra up to 30 eV of ZrN and Zr excited by 2000 eV, 25 μA primary electron beam are shown in figure 1. When magnified fifty-fold, the pure metal Zr(4p)Zr(4d)Zr(4d) Auger transition can be seen at 23 eV. This feature disappears in the stoichiometric nitride, just as was previously observed in the nitriding of Ti and V [2, 3]. A small feature which would peak at about 6 eV in the ZrN $N(E)$ spectrum is just discernible, and this feature must originate in the N(2s)N(2p)Zr(4d) Auger process, where N(2p) represents the hybridized N(2p) and Zr(4d) feature in the valence band density of states of ZrN [5]. The equivalent feature in the spectra of TiN and VN occurs at the same energy and has been discussed previously [4]. The present paper is concerned with the very large feature in the ZrN spectrum which has a minimum in the derivative spectrum close to 3 eV. This feature is so close to the peak in the secondary electron distribution, just above the inflection point, that we will not attempt any background subtraction procedures in order to obtain the intensity in the $N(E)$ mode. The intensity will be measured simply as the peak-to-peak height in the derivative spectrum. However, one could visualize the pure metal spectrum as satisfactorily approximating the secondary electron background for the ZrN spectrum, and the procedures which proved successful in our earlier studies on VN [3] may be applicable, even at this extremely low energy.

3.2. Dependence of the amplitude of the 3 eV feature on nitrogen concentration

A minimum requirement for the association of the large 3 eV feature with the nitride structure is that it scale with the nitrogen content of the surface film. The stoichiometry of the nitride surface film was varied by argon ion sputtering. Ion beam induced

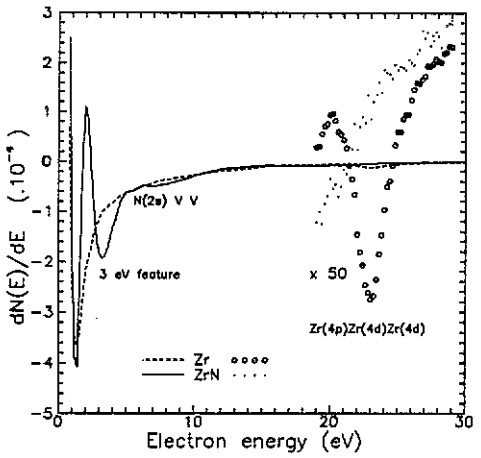

Figure 1. Derivative Auger spectra for Zr and ZrN in the energy range 0 to 30 eV. The data in the energy interval 19 to 29 eV are also displayed with the amplitude scale expanded by a factor of 50 to show the 'metal' Zr(4p)Zr(4d)Zr(4d) Auger transition at 23 eV, and its absence in the nitride spectrum. Evidence for the N(2s)VV transition previously observed in TiN and VN [4] can be seen near 6 eV. The present work focusses on the large feature in the ZrN spectrum with a maximum negative excursion at 3 eV.

processes such as ion beam mixing and radiation enhanced diffusion will lead to a homogenization of the nitrogen content throughout the penetration depth of the 2 keV argon ion beam. In figure 2 the peak-to-peak amplitude of the 3 eV feature is plotted against the amplitude of the nitrogen KLL peak at 384 eV, giving clear evidence that the intensity of the low energy feature is proportional to the nitrogen concentration. The non-linearity of the relationship should not be taken as significant since the steepness of the background for the low energy feature will guarantee that the intensity of this feature will be a non-linear function of the peak-to-peak amplitude.

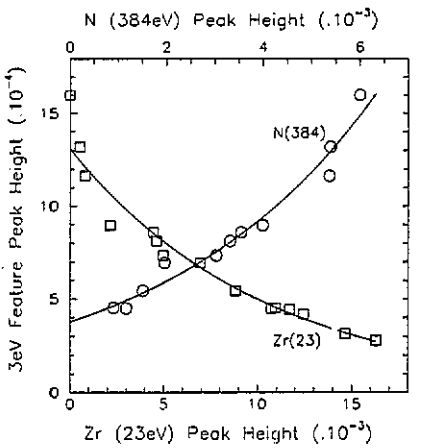

Figure 2. The variation in peak to peak amplitude of the 3 eV feature seen in figure 1 with nitrogen concentration, as measured by the N (KLL) peak height, and with the concentration of unoccupied octahedral holes, as measured by the amplitude of the Zr 'metal' peak at 23 eV.

The intensity of the Zr(4p)Zr(4d)Zr(4d) Auger peak at 23 eV will be proportional to the number of unoccupied octahedral holes in the ZrN structure, by analogy with the behaviour of the equivalent MMM transitions in TiN and VN [2, 3]. If the 3 eV feature is identified with the nitrogen content in the film, then its amplitude should decrease with the increase in the number of unoccupied holes in the structure. Thus the decrease in amplitude of the 3 eV peak with the increasing amplitude of the metal peak at 23 eV, shown in figure 2, is also consistent with the assignment of the 3 eV feature to the nitride, i.e. occupied octahedral holes.

3.3. Dependence of the amplitude of the 3 eV feature on argon gas pressure

One unusual characteristic of the 3 eV peak in the secondary electron spectrum was the dependence of its magnitude on the argon gas pressure in the analysis chamber. This can be seen in figure 3, where the amplitude of the peak is plotted against the argon gas pressure for a cycle of increasing pressure from UHV to 10^{-4} torr and then decreasing back to UHV. There are two notable features of these results. Firstly, the amplitude remains constant until about 10^{-5} torr and then falls dramatically, and secondly, the behaviour is reversible. The explanation would seem to require a reversible physical adsorption of gas, and extreme surface sensitivity of the 3 eV feature.

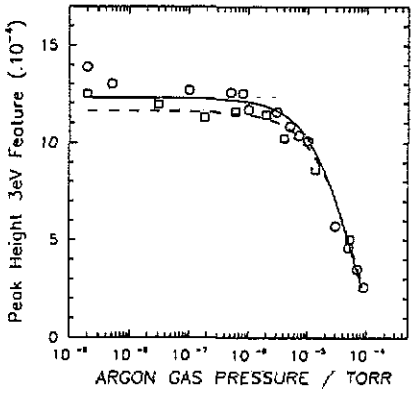

Figure 3. The change in the amplitude of the 3 eV feature with the pressure of argon gas in the UHV chamber. Data are shown with increasing (O) and decreasing, (□) pressure for a complete cycle from UHV to 10^{-4} torr to UHV. The solid and dashed curves are exponential fits to the data for increasing and decreasing pressure, respectively. The effect is reversible.

The Auger spectra were essentially unchanged during the cycle shown in figure 3, with the impurity peaks remaining at the noise level. The amount of argon physisorbed at 10^{-4} torr and 300 K should be entirely negligible, since even at 77 K, about 10 degrees below the normal boiling point, a fractional coverage of only 0.01 has been reported on zirconium [6]. Calculations based on reasonable estimates of the enthapy of adsorption are consistent with this conclusion. The most likely explanation is that some minor impurity in the argon gas is physisorbing on the surface. Since no new features were detected in the Auger spectrum, we conclude that this adsorption is either extremely weak and therefore very efficient in eliminating the process leading to the 3 eV feature, or the adsorbate is hydrogen and therefore undetectable by AES. The reversibility of the effect does not exclude hydrogen adsorption as a possible

explanation, even though it is expected to chemisorb on the surface. It is known that hydrogen diffuses into zirconium even at room temperature [7], and therefore the surface concentration will be determined by a balance between the rates of adsorption, proportional to the gas pressure, and diffusion. Thus the reversibility of the effect can still be understood. An experiment to directly test the effect of hydrogen adsorption on the amplitude of the 3 eV feature, to be described in the following section, was complicated by the oxidation of the nitride surface.

3.4. Effect of hydrogen gas on the 3 eV feature

The variation in magnitude of the large feature in the low-energy secondary electron spectrum of ZrN with a cycle of increasing and decreasing H_2 pressure followed by a short Ar ion sputter is shown in figure 4(*b*). In its initial stages, the result of this experiment seems to confirm the proposal that adsorption of H_2 impurity in the system is responsible for the elimination of the 3 eV feature on increasing the Ar gas pressure. The peak height begins to decrease for H_2 pressures in the 10^{-7} range, two orders of magnitude lower than observed with Ar gas, and has fallen by a factor of 0.5 at a H_2 pressure of 4×10^{-6} torr. Thereafter, the peak height begins to increase with increasing H_2 pressure. On reducing the H_2 gas pressure the 3 eV peak height increases even more rapidly, until at 6×10^{-9} torr it has become eight times its initial value. Selected low energy electron spectra throughout this cycle are shown in figure 4(c), in which the initial surface is shown with a full line spectrum, and succeeding spectra are displayed with dashed lines of decreasing length. The final spectrum, at 6×10^{-9} torr, can be seen to be so large as to dominate the low energy electron spectrum. The peak heights of the N and O KLL Auger peaks taken periodically during this cycle of increasing and decreasing H_2 pressure are shown in figure 4(*a*) and allow an interpretation of these surprising results. It can be seen that there is a steady decrease in the size of the nitrogen peak and a corresponding increase in that of oxygen. Presumably this occurs by the formation of water by the reaction of H_2 gas with oxide components of the UHV system, which then oxidizes the ZrN surface. The oxidized surface gives a much larger feature than the initial nitride, which is affected in the same way by adsorption of H_2 gas, and thus explaining the large increase in the amplitude of this feature on pumping out the H_2 gas. That the oxide is restricted to the surface region is suggested by the result of a brief Ar ion sputter, which reduces the oxygen peak to near its background level and increases the amplitude of the nitrogen peak.

3.5. Dependence of the 3 eV feature on primary beam energy

In the unlikely event that the 3 eV peak was a primary beam energy loss feature, or was a result of some artefact in the primary beam, such as elastic scattering of a minor low energy component in the primary beam caused by the scattering off an electrode in the electron gun, then the feature should show some dependence on the primary beam energy. Results for the dependence of the low energy peak characteristics on primary electron beam energy are shown in figure 5(*a*) and (*b*) for films with high and low nitrogen contents, respectively. In figure 5(*a*) spectra for beam energies of 2000 and 500 eV are shown with the former scaled by 0.2 times to compensate for the increased beam current used. It can be seen that the lower the primary beam energy, and therefore the smaller the penetration depth and greater the fraction of the secondary electron flux produced at the surface, the larger is the low energy feature. This inverse relationship between the amplitude of the 3 eV feature and the primary beam energy

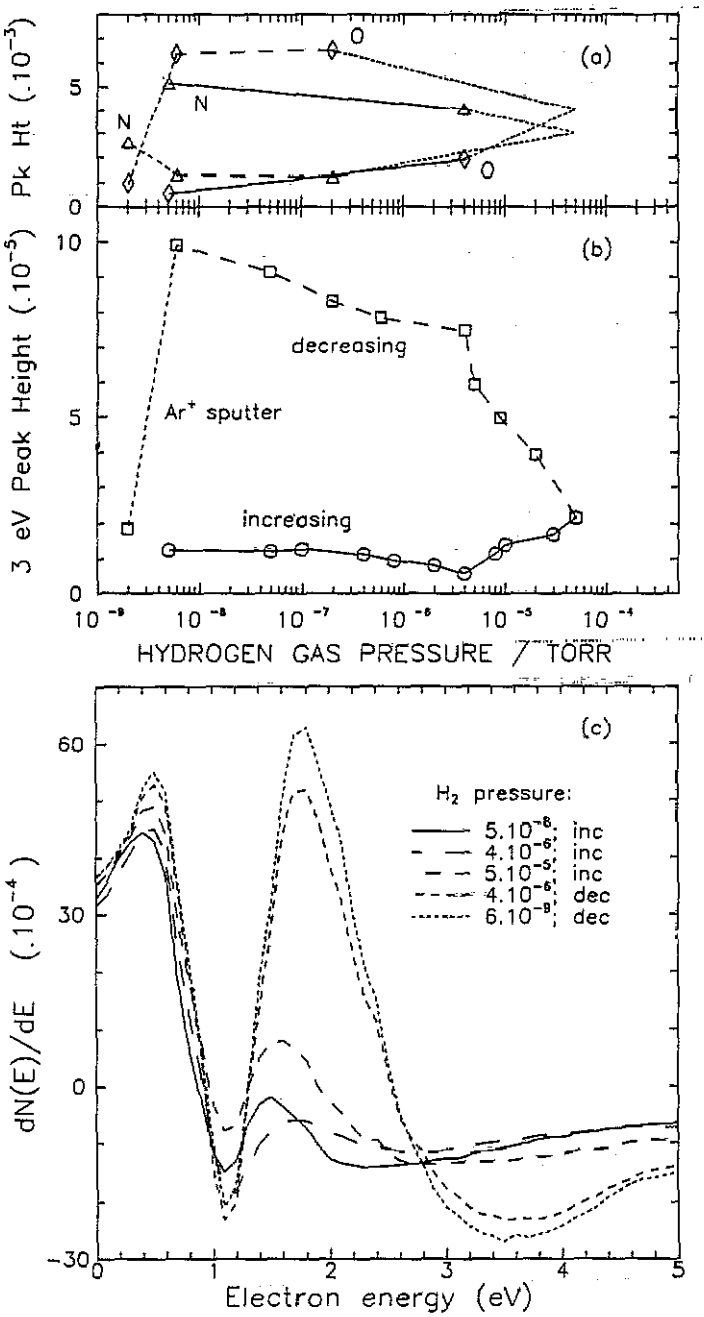

Figure 4. (*b*) shows the variation in amplitude of the 3 eV feature during a cycle in H_2 gas pressure from UHV to 5×10^{-5} torr to UHV, followed by a brief Ar ion sputter. The low (0–5 eV) secondary electron spectra at several points during this cycle are shown in (*c*), and the amplitudes of the N (KLL) and O (KLL) Auger peaks are shown in (*a*).

can also been seen in figure 5(*b*) for which the same primary beam current of 5 μA was used throughout. The feature is not an artefact, but a genuine characteristic property

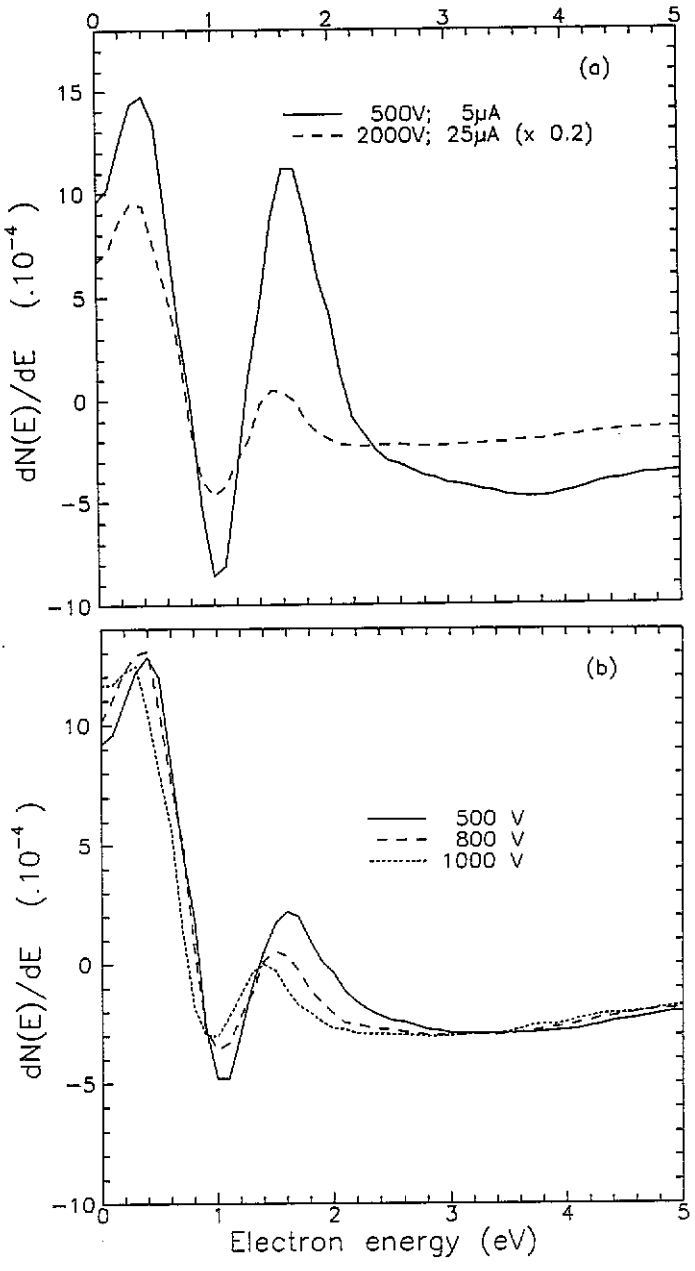

Figure 5. The effect of changes in primary electron beam energy on the 3 eV feature for nitride samples with (*a*) high, and (*b*) low nitrogen content. In (*a*) the 2000 V spectrum has been scaled by a factor of 0.2 to compensate for the higher beam current used in this experiment. The spectra in (*b*) were all obtained with identical, 5 μA, beam currents. The peak position is relatively insensitive to change in primary beam energy, but the intensity increases with decreasing beam voltage.

of the low energy secondary electron spectrum.

3.6. Dependence on crystal orientation

The original Zr sample rod from which the sample disc was cut had been subjected to a high temperature anneal and thus, although polycrystalline, it was found to have large single crystal grains approximately 1 mm in size. This is larger than the diameter of the electron beam used and permits a crude determination of the effect of crystal orientation on the amplitude of the low energy feature. The variation in amplitude of the 3 eV feature at 1 mm intervals in a line scan across the Zr sample following nitrogen adsorption for 10 minutes at 300 K and 1×10^{-6} torr is shown in figure 6(a). There is a clear dependence of this amplitude on sample position and therefore, we conclude, on crystal orientation, since there was no variation in the N (KLL) amplitude or impurity level across the sample. Representative spectra with low and high peak heights are shown in figure 6(a) and (c). In addition to the crystal orientation dependence, it should be noted that these results illustrate our observation that nitrogen adsorption, as well as nitrogen ion implantation, produce this characteristic low energy feature in the secondary electron specturm.

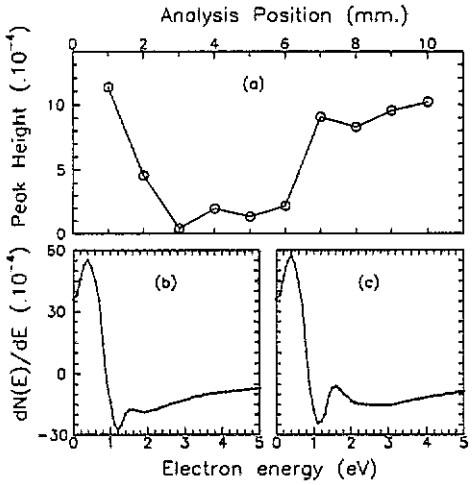

Figure 6. (a) The variation in amplitude of the 3 eV feature in a line scan across a Zr sample with chemisorbed nitrogen. Representative low energy electron spectra at 4 and 8 mm are shown in (b) and (c) respectively.

4. Discussion

The very strong feature observed with a maximum negative excursion in the derivative spectrum near 3 eV could have its origin in several processes. We will consider the following possible assignments for the feature: First to an Auger process, then to a work-function-shifted component in the secondary electron spectrum and, finally, to a surface-resonance-enhanced secondary electron emission process.

There exists an Auger process which would produce electrons with a characteristic energy near 3 eV, namely the Zr(4p)N(2s)N(2p) transition, where N(2p) signifies the hybridized N(2p) and Zr(4d) feature in the valence band density of states. The energy of such electrons can be estimated in the usual way by the relation:

$$E \cong E[\mathrm{Zr}(4p)] - E[\mathrm{N}(2s)] - E[\mathrm{N}(2p)] - U_{\mathrm{eff}} - \phi$$

or

$$E \cong 8.0 - U_{\text{eff}} - \phi$$

where the following electron binding energies have been used; Zr(4p) = 29.7; N(2s) = 16.7; and N(2p) = 5.0 eV, [8]. This assignment would give good agreement with the observed energy with reasonable values for the hole-hole interaction energy, U_{eff}, and collector work function, ϕ. It is also consistent with the dependence of the intensity of the signal on nitrogen concentration, and independence of the peak position on primary beam energy and the increase in magnitude observed with decreased beam voltage, since in all cases the primary beam energy is greatly in excess of three times the Zr(4p) ionization energy. Furthermore, the fact that the signal is extremely large can perhaps be understood in view of the estimated escape depth of 50 monolayers for such low energy electrons [9]. The characteristic properties which are at odds with this interpretation as an Auger feature are, firstly, the extreme sensitivity to weak reversible adsorption of either hydrogen or an undetectable concentration of some other impurity, and secondly, the strong dependence on crystal orientation.

The observation that on oxidation, figure 4(*c*), or at low primary beam current, figure 5(*a*), the strong feature can become a dominant component in the total secondary electron emission suggests that it is simply a varying fraction of the total secondary flux which has been shifted by the change in the work function of the surface. There are several problems with this model. Why is the peak position largely independent of composition when it is well known that the work function shift is a strong function of composition [7]? Since we always observe an unperturbed as well as a shifted peak in the electron energy distribution, one could argue that the nitrided or oxidized surfaces are distributed spatially as patches of constant work function which grow in area with increasing concentration. However, why does the peak appear at the same position for the oxidized surface as in the nitride when the work function changes are in the opposite directions for the two cases, + 0.6 eV for O and −0.15 eV for N [7]? Why is the peak in the secondary electron distribution shifted to higher energies for the oxidized surface when the work function is actually increased? The dependence of the intensity, rather than position, on crystal orientation is also difficult to understand with this model, and, finally, why the extreme sensitivity to surface impurities?

There are several studies reported in the literature which have features in common with the present observations, and provide some clues as to their interpretation. Seah [10] in a study of the secondary electron spectrum from Cu, Ag and Au observed characteristic peaks close to 13 eV in the normal emission spectrum. For the case of Ag, the intensity of this feature was greater for Ag(111) single crystal film than for a polycrystalline sample, and model calculations led to the suggestion that this emission originated in the decay of a surface-related excited state. Models based on small angle inelastic scattering of the primary beam followed by elastic scattering, a diffracted inelastic peak, or based on the bulk band structure were found to be inconsistent with the experimental observations. Willis *et al* [11] have observed the angle-resolved secondary electron emission normal to a W(110) crystal, and found that oxidation of the surface produced a new peak at 3 eV kinetic energy which was attributed to an adsorbate-induced surface resonance lying above the vacuum level. Feuerbacher and Fitton [12] have shown that the intrinsic surface state in the occupied density of states of W(100) at 0.4 eV below the Fermi level is extremely sensitive to adsorbed gas. Monitoring this state by UV photoemission spectroscopy they found that it completely

disappeared after an exposure to H_2 gas of 0.4 Langmuir, corresponding to a fraction of a monolayer coverage. There seems every reason to believe that extrinsic, unoccupied, states would show a similar sensitivity to adsorbed gases. The energy of the adsorbate induced surface resonance required to account for the present observations on nitrided Zr should be located about 2 eV above the vacuum level and it may be possible to detect this state in electron energy loss spectra. A loss feature observed at 6.2 eV in ZrN [5] could arise from transitions from the Zr(4d) state, 0.35 eV below the Fermi energy, to the proposed unoccupied state. For comparison with the larger features observed for the oxidized surface, figure 4(*c*), Palacio *et al* [13] have published EELS data for clean and oxidized Zr. They observed energy loss peaks at 6.3 and 7.8 eV for the clean and oxidized surfaces respectively, which, given reasonable values for the work function of 4.5 ± 0.5 eV, are consistent with the requirements of the model. The change in magnitude of the energy loss energy on oxidation is in agreement with the peak energy difference observed in figure 4(*c*). It is worth noting that in the published secondary electron emission spectra of Palacio *et al* for the early stages of oxidation of Zr, we can see two features at the same energies as those observed in the present work, although the authors make no comment on their presence or origin.

In conclusion, the strong dependence of the secondary electron features observed for both ZrN and its oxidized surface on crystal orientation and its sensitivity to reversible adsorption of gases, point to an origin in an adsorbate induced surface resonance lying just above the vacuum level. However, a contribution from other processes, such as those discussed earlier, cannot be ruled out. Further understanding of these processes must await angle-resolved studies on well characterized single crystal surfaces.

Acknowledgments

The authors are grateful for the support provided by the award of a Pao Yu-kong and Pao Zhao-long Scholarship to Yan Chen.

References

[1] Toth L E 1971 *Transition Metal Carbides and Nitrides* (New York: Academic)
[2] Dawson P T and Tzatzov K K 1986 *Surf. Sci.* **171** 239
[3] Dawson P T and Tzatzov K K 1990 *Surf. Sci.* **234** 339
[4] Dawson P T and Tzatzov K K 1991 *Surf. Sci.* **249** 223
[5] Schubert W K, Shelton R N and Wolf E L 1981 *Phys. Rev.* B **24** 6278
[6] Hansen N 1962 *Vakuum-Tech.* **3** 70
[7] Foord J S, Goddard P J and Lambert R M 1980 *Surf. Sci.* **94** 339
[8] Höchst H, Bringans R D, Steiner P and Wolf Th 1982 *Phys. Rev.* B **25** 7183
[9] Seah M P and Dench W A 1979 *Surf. Int. Anal.* **1** 2
[10] Seah M P 1969 *Surf. Sci.* **17** 132
[11] Willis R F, Feuerbacher B and Fitton B 1976 *Solid State Commun.* **18** 185
[12] Feuerbacher B and Fitton B 1972 *Phys. Rev. Lett.* **29** 786
[13] Palacio C, Sanz J M and Martinez-Duart J M 1987 *Surf. Sci.* **191** 385